Research in Astronomy and Astrophysics manuscript no.
(LaTeX: ImageResolution˙RAA.tex; printed on October 29, 2015; 0:24)

arXiv:1510.08227v1 [astro-ph.IM] 28 Oct 2015

A Statistical Definition of Image Resolution Based on the Correlation of Pixels

Jian-Feng Zhou[1,2]

[1] Department of Engineering Physics and Center for Astrophysics, Tsinghua University, Beijing 100084, China; *zhoujf@tsinghua.edu.cn*

[2] Key Laboratory of Particle & Radiation Imaging (Tsinghua University), Ministry of Education, Beijing 100084, China.

Abstract Resolution, usually defined by the Rayleigh criterion or the Full Width at Half Maximum of a Point Spread Function, is a basic property of an image. Here, we present a new statistical definition of image resolution based on the cross-correlation properties of the pixels in an image. It is shown that the new definition of image resolution depends not only on the PSF of an imaging device, but also on the signal-to-noise ratio of the data and on the structures of an object. In an image, the resolution does not have to be uniform. Our new definition is also suitable for the interpretation of the result of a deconvolution. We illustrate this, in this paper, with a Wiener deconvolution. It is found that weak structures can be extracted from low signal-to-noise ratio data, but with low resolution; a high-resolution image was obtained from high signal-to-noise ratio data after a Wiener deconvolution. The new definition can also be used to compare various deconvolution algorithms on their processing effects, such as resolution, sensitivity and sidelobe level, etc.

Key words: methods: statistical — techniques: image processing — techniques: high angular resolution

1 INTRODUCTION

Resolution, or spatial resolution, or angular resolution, describes the ability of an imaging device to distinguish small details of an object. In optical devices such as an optical or radio telescope, a microscope etc., Airy pattern is the description of the best focused spot of light that a perfect lens with a circular aperture can make, limited by the diffraction of light. The resolution of such imaging systems can be estimated by the Rayleigh criterion: two point sources are regarded as just resolved when the principal diffraction maximum of one image coincides with the first minimum of the other (Born & Wolf 1999). For a general imaging system, like a coded-mask, an interferometry, etc., the FWHM (Full Width at Half Maximum) of its PSF

In practice, one is interested more in the resolution of an image itself than in that of an imaging system. An observed image is related to the properties of its imaging system, but also to the intensity distribution of an object, and to additive noise. Therefore, the resolution of an image is not only influenced by the PSF of an imaging system, but also by the structures of the object and noise. It is useful to find a new definition that can be used for directly estimating the resolution of an observed image.

Super-resolution images can be obtained through various methods. Irani and Peleg (1991) proposed an algorithm based on image registration where a series of low-resolution images were used and their relative displacements were known accurately. Even for one single observed image blurred by an imaging system, deconvolution or blind deconvolution can be used for improving the resolution (Conchello 1998). Fourier ring correlation (FRC) (Saxton & Baumeister 1982; Nieuwenhuizen et al. 2013; Banterle et al. 2013), which can be computed directly from an image, was applied to estimate the resolution of optical nanoscopy (or super-resolution microscopy).

In principle, a proper quantitive definition of resolution needs detailed information about the relationship of the pixels of an image. So far, there is still no such kind of definition. In this paper, a new definition of image resolution based on the statistical properties of observed images is proposed. In section 2, some basic factors that influence image resolution are introduced. The relationship between the correlation of pixels and image resolution is indicated in section 3, and then a new definition of image resolution is presented there. In section 4, Wiener deconvolution is used to demonstrate super-resolution and dynamic resolution under different signal-to-noise ratio conditions . Finally, a discussion and conclusions are presented in section 5 and 6.

2 FACTORS RELATED TO IMAGE RESOLUTION

A linear imaging system can be described by the following equation

$$\mathbf{d} = \mathbf{o} \otimes \mathbf{p} + \mathbf{n}, \tag{1}$$

where $\mathbf{d}$ is an observed image, $\mathbf{o}$ is an object or a scene, $\mathbf{p}$ is the PSF of the system, $\mathbf{n}$ is additive noise, and $\otimes$ denotes convolution.

In the classical definition of image resolution, only the properties of a PSF is considered, whereas a real observed image is not only influenced by the PSF, but also by the structures of an object and noise.

2.1 Point Spread Function

As mentioned in the introduction, the Rayleigh criterion or the FWHM of a PSF can be used as a definition of image resolution. But these definitions are not suitable for all kinds of PSFs. Some PSFs' shapes are rather strange and complex. They often have negative minimum, which has no physical meaning, and strong sidelobes that make central beam insignificant. For example, the PSF of a coded-mask imaging system usually has big sparse sidelobes (Ubertini et al. 2003). Also, in speckle interferometry, although high resolution information is preserved, the PSF in each frame with short exposure has large spread area and a strong fluctuating structure due to atmospheric turbulence, with no obvious main beam (Fried 1966,

2.2 Object Structures

It is shown in (1) that the intensity distribution of object **O** has an influence on the observed image.

Due to the stochastic properties and to the particle nature of light, there is always fluctuation in an observed image: this is called shot noise (Blanter & B$\acute{}$uttiker 2000). The brighter the source, the stronger the noise. Such fluctuation can usually be described by Poisson distribution. If the photon number in a pixel is N, then the relative fluctuation level is proportional to $1/\sqrt{N}$.

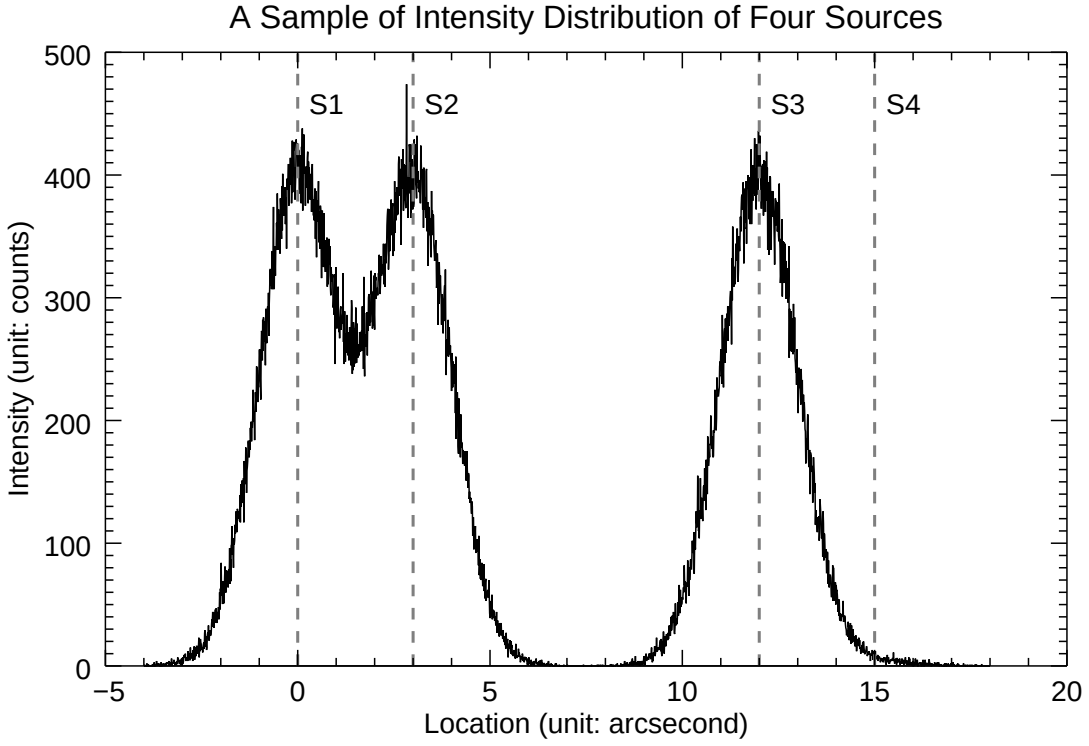

Fig. 1 Example showing how the structure of an object affects the resolution and detectability when shot noise is taken into account.

In a real observed image, the exposure time is limited. Therefore, faint structures will generally be drown in the large fluctuations of nearby bright structures because of their large shot noise.

Let's use an example to show how the structure of an object affects the resolution of an image (see Fig. 1). Here, a normal Gaussian PSF with FWHM of 2.3 arcsecond is used. Four point sources are located at position 0, 3, 12 and 15 arcseconds and denoted by S1, S2, S3 and S4 respectively. S1, S2 and S3 have an identical number of received photons, which is 10^5. S4 is much weaker and has 10^3 photons. Since the distances between S1 and S2, as well as S3 and S4 are greater than the FWHM of the PSF, they should be resolvable under the classical definition of image resolution. Fig. 1 clearly shows that S1 and S2 are resolved. However, S4 is shadowed by its neighboring strong source S3.

2.3 Additive Noise

An image's additive noise, sometimes known as "dark shot noise" (MacDonald 2006) or "dark-current shot

noise is an undesirable by-product of the physical image capture process. In a dim scene, the additive noise (Tuzlukov 2010) will be dominant and has an influence similar to that of shot noise . It may conceal faint sources and add spurious and extraneous information.

3 CORRELATION AND IMAGE RESOLUTION

Correlation is a mathematical term that describes a relationship between two random variables. There are several definitions of correlation. Among them is Pearson's definition (Pearson 1985), which captures the linear relationship between two random variables and is the most popular.

For an observed image, the counts of pixels are random variables whose statistics can be used to study the resolution property of the image. The means of these variables match a distribution which can be described by (1). The classical definitions of image resolution are relevant to this distribution. In this paper, quadratic statistics, and especially correlation coefficients are used for analyzing the resolution property of an image.

3.1 Correlation Induced by Imaging Devices

Signals emitted from different objects or from different parts of the same object are usually incoherent. This property can be mathematically described by Pearson's cross-correlation coefficient. If S_1 and S_2 are two signals from different places, then the correlation coefficient (abbreviated as CC hereafter) between them is $\rho(S_1, S_2) = 0$.

For an imaging device, if the size of a pixel in its detector is much larger than the FWHM of the PSF, then different pixels in a received image represent different parts of the object or scene. In this situation, $\rho(R_1, R_2) = 0$, where R_1 and R_2 represent the signals from two pixels, i.e., the signals from different pixels are incoherent. If the size of a pixel is less than the FWHM of the PSF, however, the signals from different pixels are generally coherent.

Let's use a simulated one-dimension example to demonstrate the influence of an imaging device on the CC. The object (see Fig. 2) consists of two point sources and one extended source. The point sources are located at pixels 120 and 140 respectively and have the same brightness of 80000 counts/s. The extended source resides in [280, 380] has a brightness of 200 counts/s.

First, we choose a situation where the PSF is smaller than a pixel of the detector, A series of simulated observed images are obtained. One sample where $1\,\mathrm{pixel} = 1\,\mathrm{arcsecond}$ is shown in Fig. 3 (top plot). The cross-correlation coefficient matrix can be calculated and is shown in Fig. 4. Three coefficient curves related to specific pixels are extracted from that matrix and shown in Fig. 3 (bottom plot).

Fig. 3 shows that all of three CC curves are essentially δ-functions, which means that there is no correlation between any pair of pixels in the image. The same is also true for the CC matrix (see Fig. 4) where only diagonal elements are equal to 1 and other elements are close to 0.

Second, we choose another situation where the PSF is larger than a pixel of the detector. A Gaussian function with $\sigma = 10$ pixels is set as the PSF of the imaging system (see the top plot in Fig. 5). 100

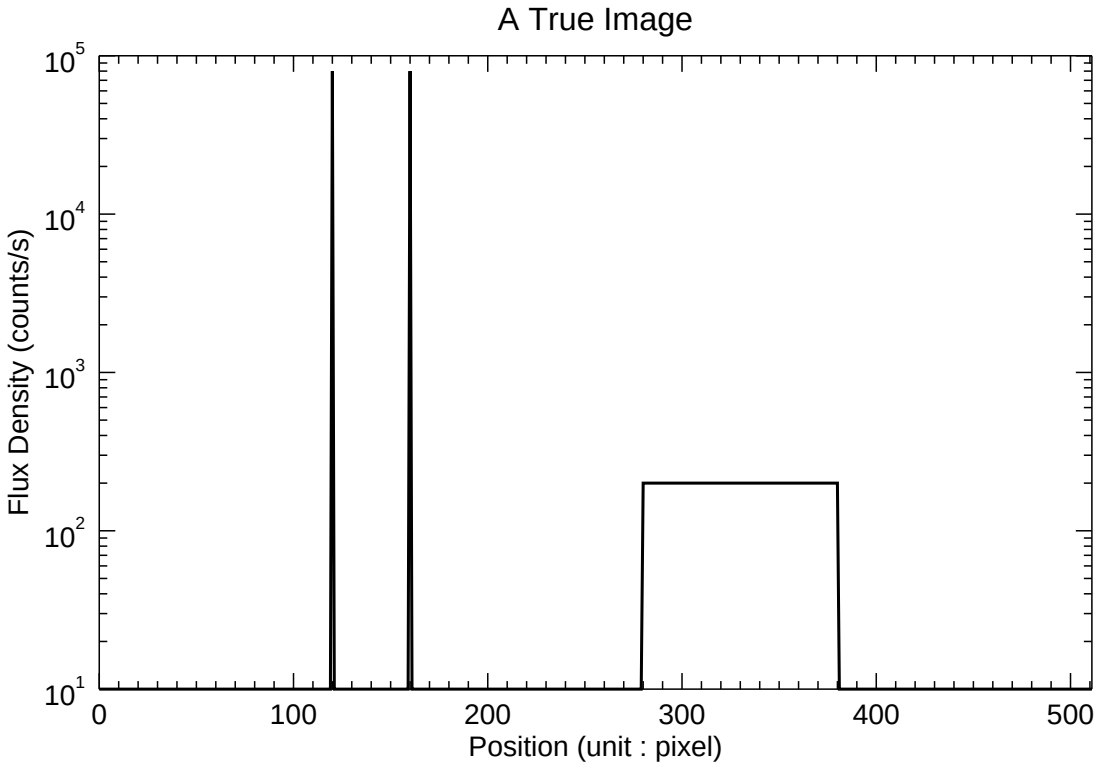

Fig. 2 Brightness distribution of a simulated object or true image.

is shown in Fig. 6. Three coefficient curves related to specific pixels 120, 160 and 330 are extracted from that matrix, as shown in Fig. 5 (bottom plot).

In the second situation, there are non-uniform extended structures in the CC matrix (see Fig. 6), which are induced by the imaging device. Fig. 5 and 6 show that the shape of CC curves depends on the structures of the object, on the PSF and on the noise level.

3.2 Statistical Definition of Image Resolution

A statistical definition of angular resolution is quite straightforward. A correlation coefficient (CC) matrix or tensor could be derived from a series of observed or deconvolved images. Next, one needs to find the background level of CCs. If there is signal in the images, the CLEAN (H$\acute{}$ogbom 1974) algorithm could be used to remove this signal from the images. Then, a CC matrix can be calculated from the residual images where only incoherent noise exists. The standard deviation of the CC matrix without its diagonal elements can be calculated. By setting a confidence level (e.g., $3\,\sigma$ level) above which the correlations between pairs of pixels are believed to be real, we are able to study the resolution properties of the images(see Fig. 7).

A quantitive definition of resolution can be derived from CC curves or matrices. If the structure of the CC curves or matrices is simple, just like those shown in Fig. 7, the FWHMs of the curves can define the resolution at the corresponding pixels. Sometimes, the structure of CC curves is quite complex, as indicated by the examples in Section 4. In this situation, it is possible to define the resolution as the FWHM of the

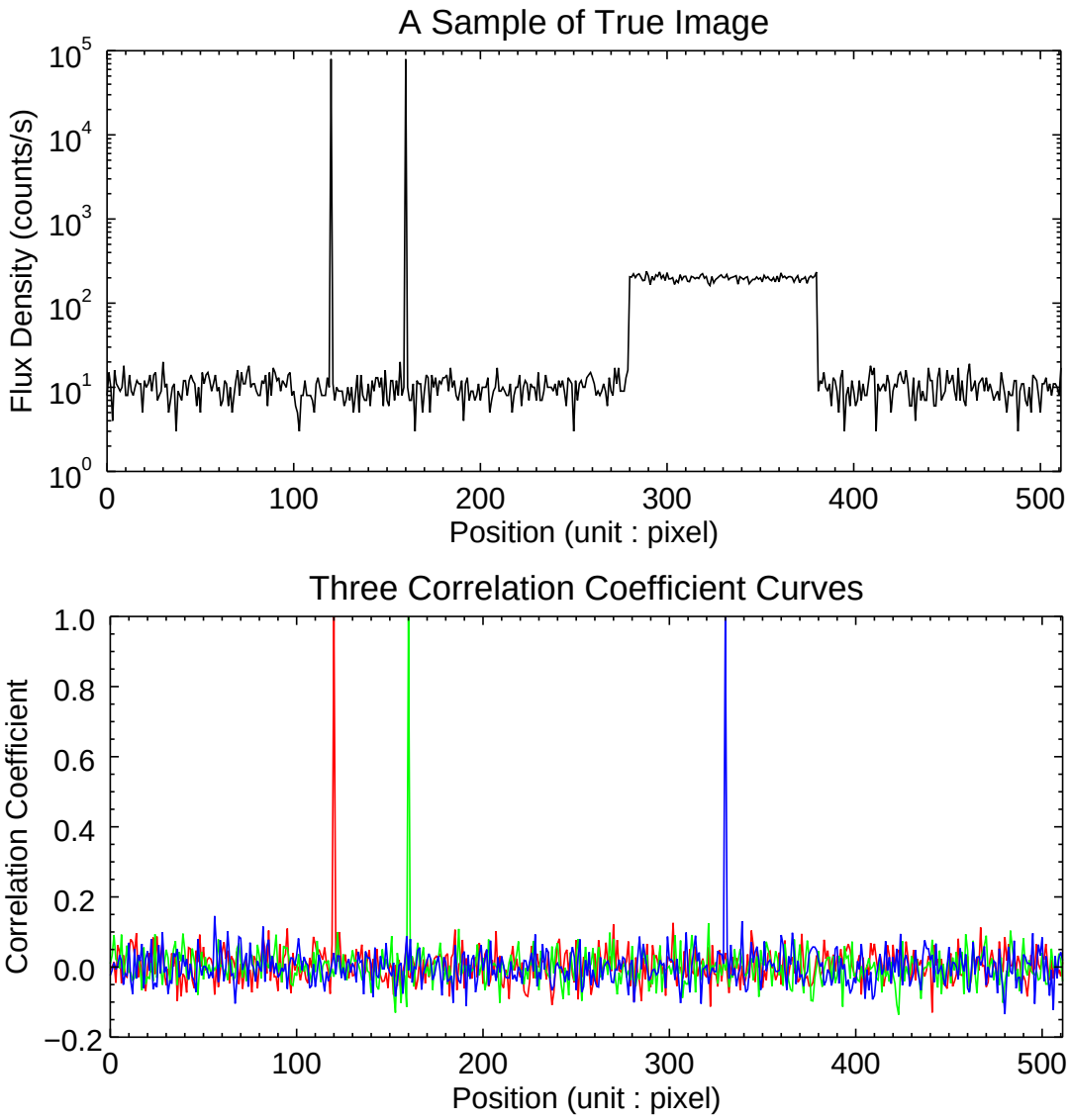

Fig. 3 One of the observed images, in a situation where the PSF is much smaller than the pixels of detector (top plot). Three correlation coefficient curves related to pixels 120 (red), 160 (green) and 330 (blue) respectively are shown in the bottom plot.

Let's use an example to demonstrate the idea of an image resolution based on the pixel correlations , with an image system that has a Gaussian PSF with $\sigma = 10\,\mathrm{px}$. The object or true image consists of four point sources and one extended source. The point sources are at positions of $120\,\mathrm{px}$, $130\,\mathrm{px}$, $220\,\mathrm{px}$ and $300\,\mathrm{px}$, with brightness of 8.0×10^4 counts/s, 8.0×10^4 counts/s, 2.0×10^4 counts/s and 4.0×10^4 counts/s respectively. The extended source ranging from $340\,\mathrm{px}$ to $440\,\mathrm{px}$ has a mean brightness of 5.0×10^3 counts/s. The additive noise is also Gaussian, with $\sigma = 2.0$ counts/s. Four CC curves are extracted from the CC matrix and are shown in Fig. 7.

As indicated in Fig. 7, the resolution in an image is variable. The CC curves related to pixel 120 and 160 has FWHM of 38 pixel and 39 pixel respectively. The CC curve related to pixel 330 has FWHM of 35 pixel. At pixel 245, the CC curve is a δ function since there is only noncoherent noise, which shows that

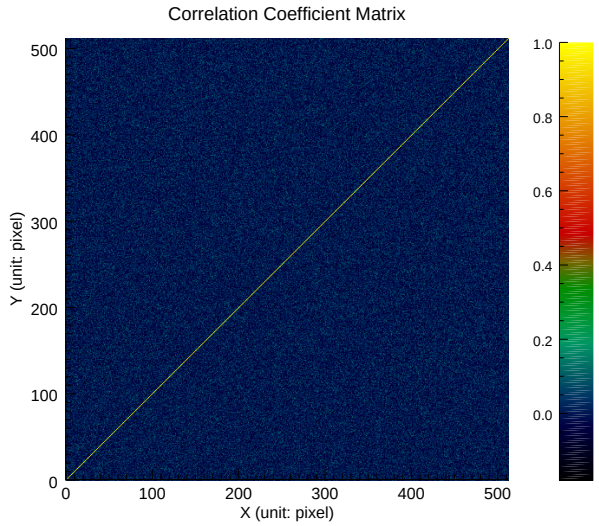

Fig. 4 The CC matrix of a series of observed images under a situation where the PSF is much smaller than the pixels of the detector.

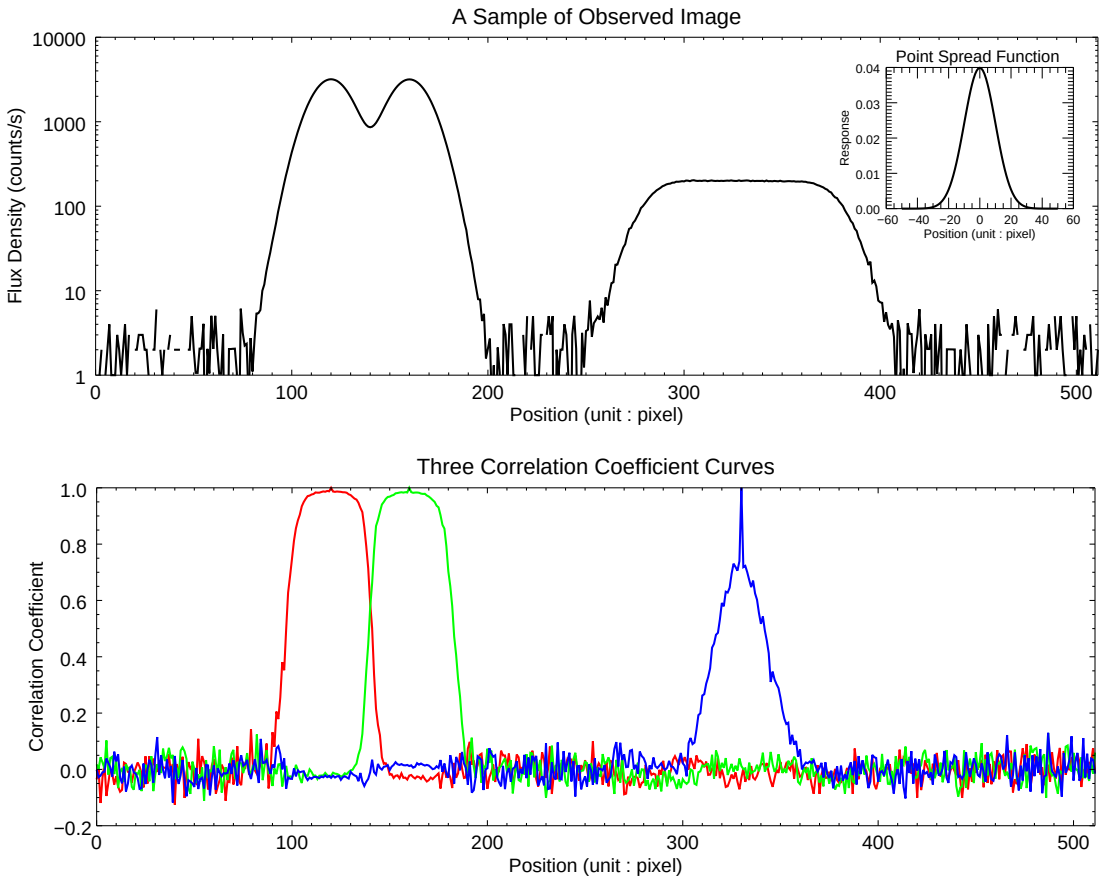

Fig. 5 One observed image, in a situation where the PSF is a Gaussian function, with $\sigma = 10$ pixels (top plot). Three CC curves, for pixels 120 (red), 160 (green) and 330 (blue) respectively are shown in the bottom plot.

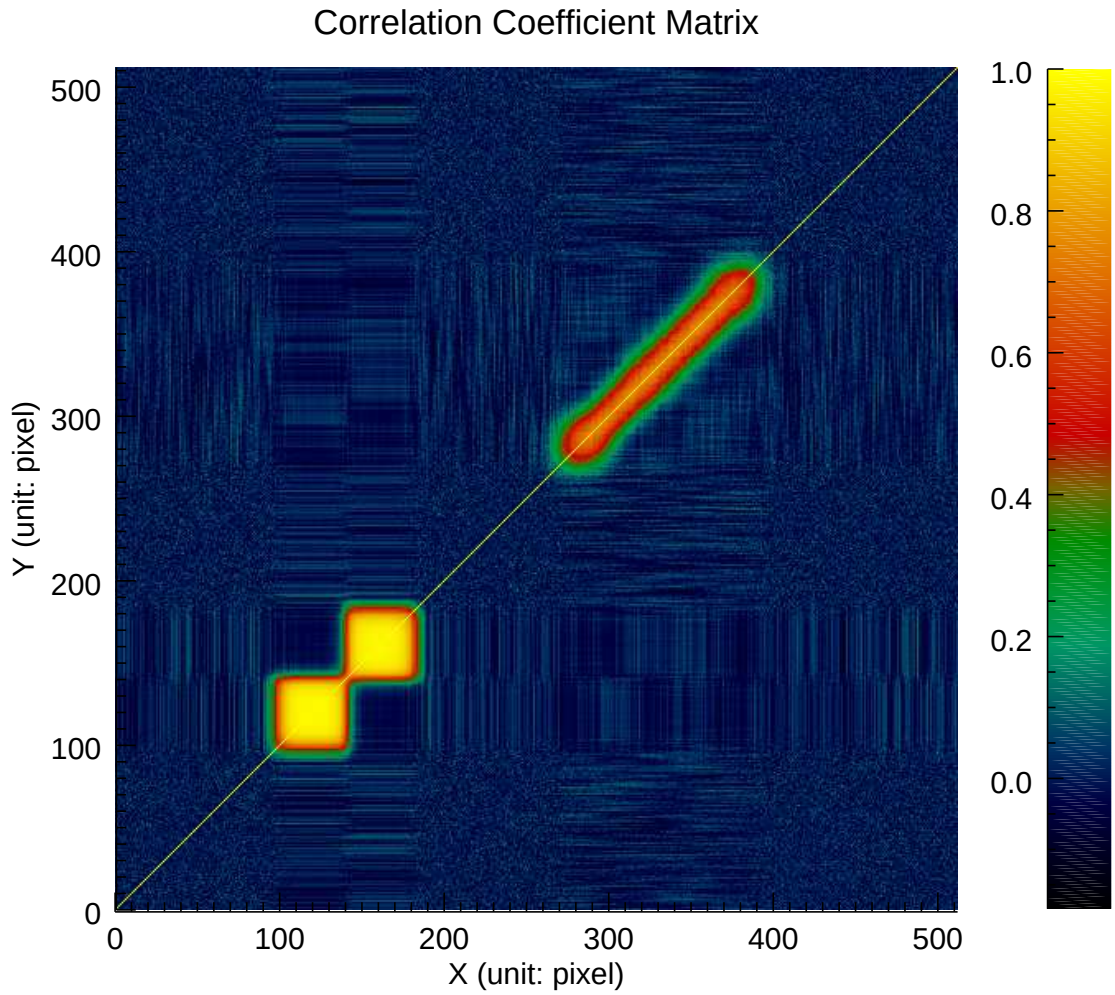

Fig. 6 The CC matrix of a series of observed images in a situation where the PSF is a Gaussian function, with $\sigma = 10$ pixels.

4 IMAGE RESOLUTION IN DECONVOLUTION

Nowadays, there are many deconvolution algorithms, such as CLEAN (H$'$ogbom 1974), Maximum Likelihood (Akaike 1998), Wiener filter (Wiener 1949), (Kalman filterKalman 1960), Maximum Entropy (Jaynes 1957), Maximum A Posteriori (DeGroot 2005) , etc. All these methods intend to provide a good estimation of the original objects. In some situation, for example with data of good quality, deconvolution can produce images with super-resolution. The super-resolution, as mentioned before, can not be described by the classical definition of resolution.

With the new definition of image resolution presented in Section 3.2, however, the super-resolution can be quantatively evaluated. We use the Wiener deconvolution for our demonstration. Other deconvolution

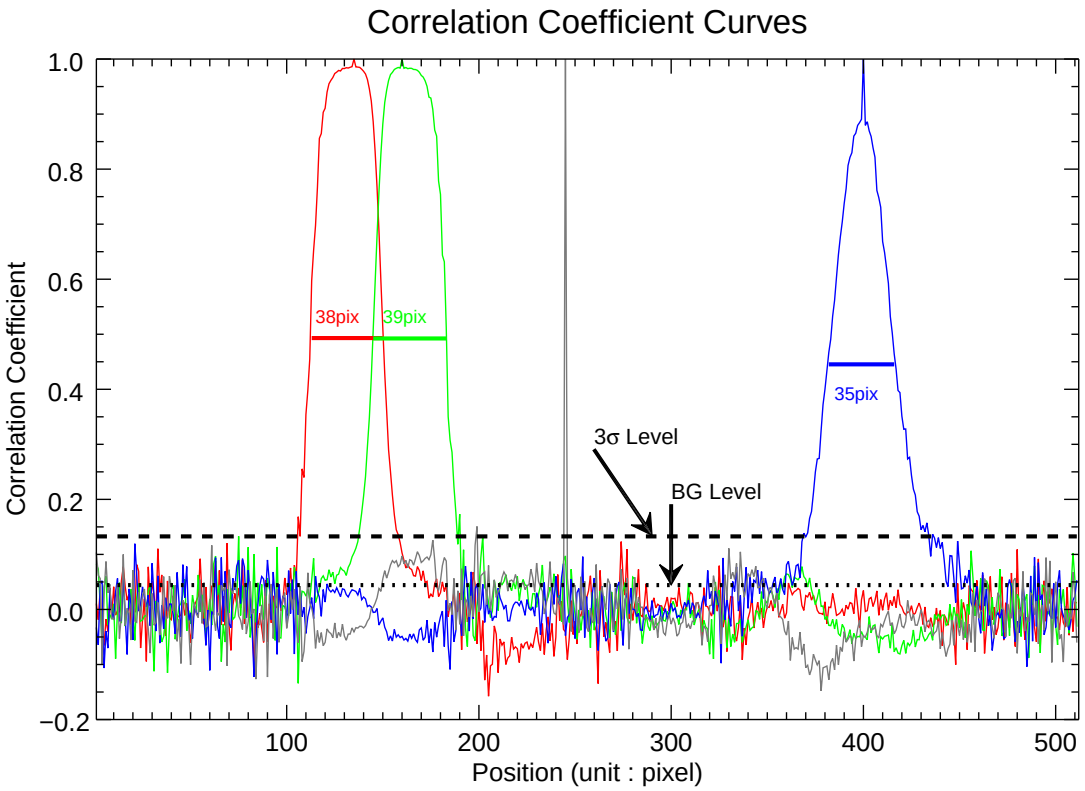

Fig. 7 An example of image resolution based on the correlation of pixels. Four CC curves related to pixels 120 (red), 160 (green), 245 (grey) and 330 (blue) respectively are extracted from the CC matrix. Background (BG) level (dotted line) and 3 σ level (dashed line) are shown in the figure too. The detailed parameters of this example are described in the third paragraph of Section 3.2.

4.1 Wiener Deconvolution

Wiener deconvolution, which is based on the Wiener filter, is a good algorithm for removing the effects of a point spread function. The main steps of the algorithm are reviewed below.

For an imaging system described in (1), the goal of the Wiener deconvolution is to find a $\mathbf{g}$ so that it is possible to estimate $\mathbf{o}$ by following operation:

$$\hat{\mathbf{o}} = \mathbf{g} \otimes \mathbf{d} \tag{2}$$

where $\hat{\mathbf{o}}$, which minimizes the mean square error, is an estimate of $\mathbf{o}$. The solution $\mathbf{g}$ can be more easily expressed in the frequency domain :

$$\mathbf{G}(f) = \frac{\mathbf{P}(f)^{*}\mathbf{O}(f)}{|\mathbf{P}(f)|^{2}\mathbf{O}(f) + \mathbf{N}(f)} \tag{3}$$

where $\mathbf{G}$ and $\mathbf{P}$ are the Fourier transforms of $\mathbf{g}$ and $\mathbf{p}$ respectively, $\mathbf{O}$ and $\mathbf{N}$ are the mean power spectral density of $\mathbf{o}$ and $\mathbf{n}$, the superscript $*$ denotes complex conjugation, f denotes frequency.

4.1.1 Example I: Low Signal-to-Noise Ratio

In this example, we use the same object (true image) as that of Section **??**. a Gaussian point spread function

Table 1 The FWHMs (in pixels) of the Main Beams of CC Curves in the Wiener Deconvolution

Position	SNR=1.3		SNR=930	
	(Observed)	(Deconvolved)	(Observed)	(Deconvolved)
120 px	N/A	22.0	35.0	19.0
220 px	N/A	25.0	32.0	16.0
400 px	N/A	24.0	34.0	14.0

generated. Each image is the convolution of a Poisson sample of the original object with the PSF, whose FWHM is about $23\,\mathrm{px}$, plus additive Gaussian noise with $\sigma = 2000$ counts/s. The corresponding SNR is about 1.3. One of the observed images is shown in Fig. 8 (middle plot). A Wiener deconvolution was applied to each sample of observed image. One deconvolved image is shown in Fig. 8 (bottom).

We produced 100 samples of observed images and Wiener deconvolved images, their CC matrices (see Fig. 9) were calculated, and CC curves at different positions (see Fig. 10) were extracted. In this situation, the noise is strong and has no correlation. In the CC matrix, there are only diagonal elements whose values equal 1.0 and with the non-diagonal elements very close to 0.0 (see Fig. 9, left plot). Therefore, there is no meaningful image resolution here.

The Wiener deconvolution is capable of suppressing noise and of detecting weak sources, as shown in Fig. 8 and Fig. 10. After deconvolution, an estimation of the object is produced, and a structure appears in the CC matrix (see Fig. 9, right plot, and Fig. 10). The FWHMs of the main beams in the CC curves are listed in Table 1. The image resolution here displays small variation, and is comparable to the FWHM of the Gaussian PSF, which is about $23\,\mathrm{px}$.

4.1.2 Example II : High Signal-to-Noise Ratio

In this example, again, we use the same object (true image) as that of Section **??**. The Gaussian noise was reduced to $\sigma = 2.0$ counts/s. The corresponding SNR is about 930.

Fig. 11 shows the object or true image (top plot), one of the observed image (middle plot) and its Wiene-deconvolved image (bottom plot). Fig. 12 shows the CC matrices of 100 observed images (left plot) and of their Wiener deconvolved images (right plot). Three pairs of CC curves at positions $120\,\mathrm{px}$, $220\,\mathrm{px}$ and $400\,\mathrm{px}$ respectively are shown in Fig. 13.

We see in Fig. 12 and 13 and Table 1 that the image resolution of observed images ranges from $32\,\mathrm{px}$ to $35\,\mathrm{px}$ is larger than the FWHM of the PSF, which is about $23\,\mathrm{px}$. How the SNR affects the image resolution will be discussed in Section 5. The table also shows that the resolution after Wiener deconvolution ranges from $14.0\,\mathrm{px}$ to $19.0\,\mathrm{px}$, which is better than the resolution of the observed images. The resolution is also less than the FWHM of the PSF, which properly indicates that Wiener deconvolution achieves super-resolution. Looking into the bottom plot in Fig. 11, we can see that two point sources at $120\,\mathrm{px}$ and $140\,\mathrm{px}$

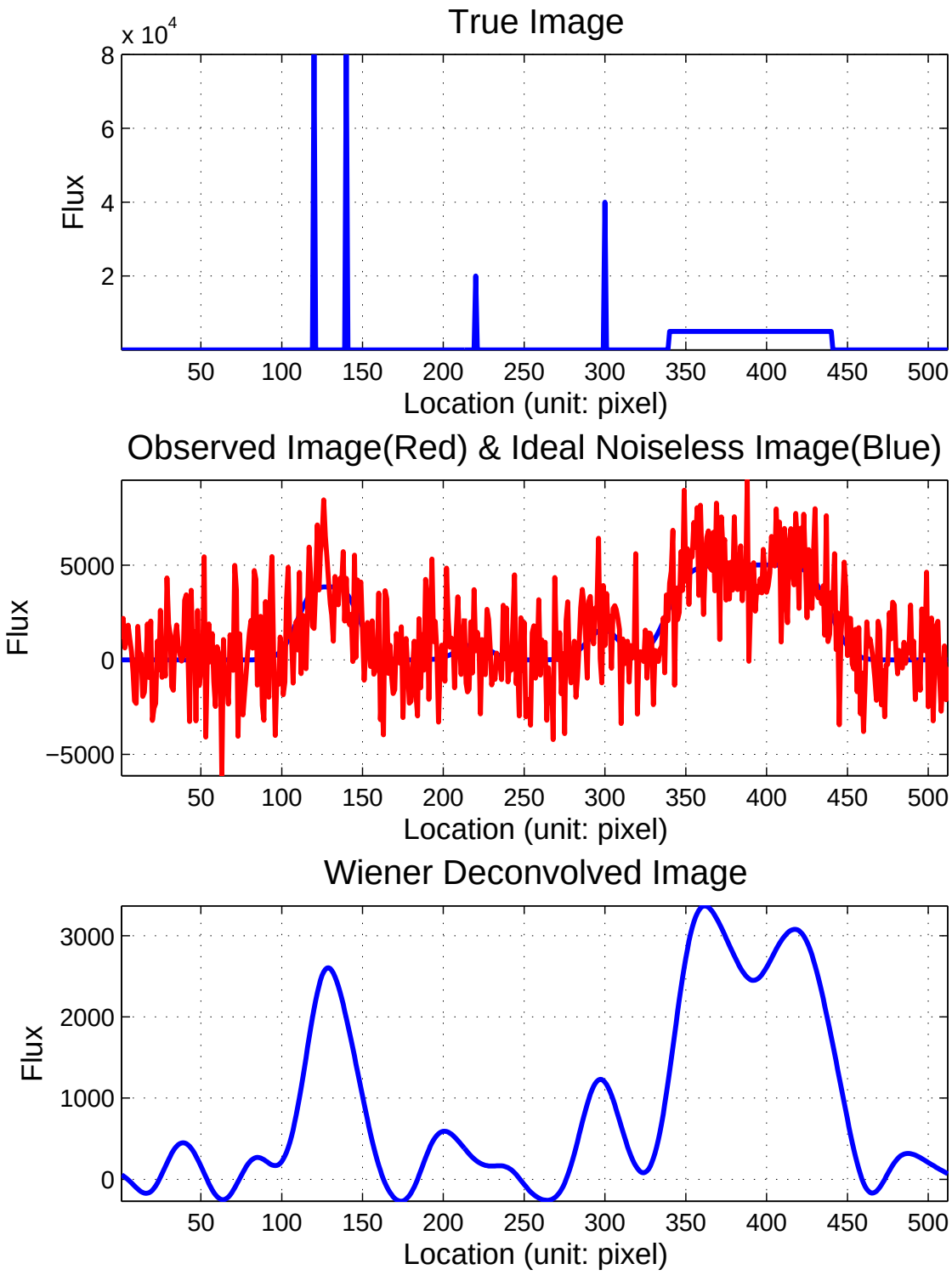

Fig. 8 The true image (top plot), the observed image as well as the ideal noiseless image (middle plot) and the Wiener deconvolved image (bottom plot) in Example I where the SNR of the observed image is about 1.3.

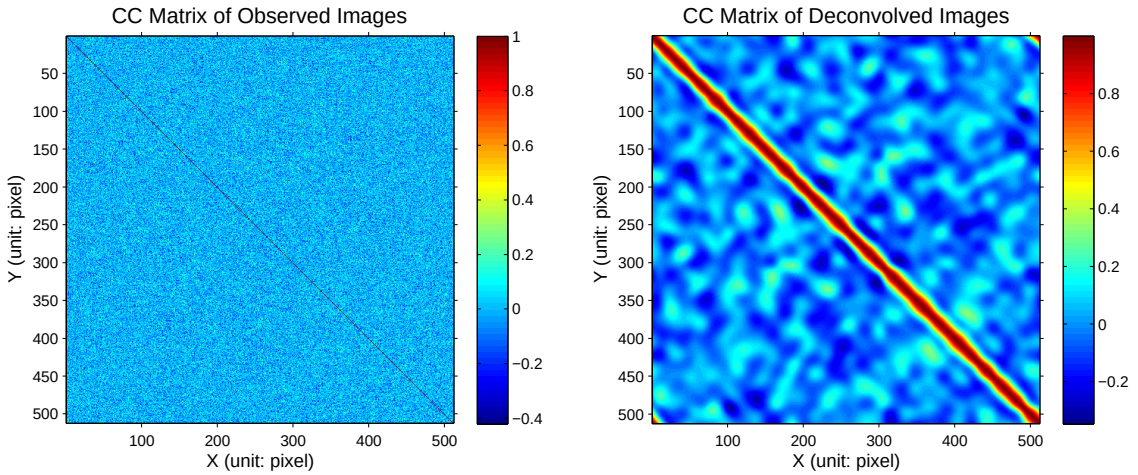

Fig. 9 CC matrices of observed images (left plot) and deconvolved images (right plot). The SNRs of the observed images are about 1.3

5 DISCUSSION

To the first order approximation, an imaging system can be described by (1). In the new definition of resolution given in this paper assumes that the objects are variable. Their variations, after convolution with a PSF, induces correlation in an observed image.

In a real imaging system, quantum mechanics controls the behavior of photons. A photon arrives at a pixel of a detector with a probability which is dominated by the normalized profile of a PSF. So, there will be no correlation in a series of real observed images. An exception is if objects are variable. Simulation shows that if a point source has a fluctuation which is larger than its intrinsic fluctuation ($1/\sqrt{N}$), then the cross-correlation coefficient curve has the shape of the PSF.

Even though the new definition in this paper doesn't describe the quantum nature of a real imaging system, it is still a powerful analytical tool that can be used for evaluating an imaging system in some special objects under some special noise levels, and also for assessing the performance of a deconvolution algorithm.

As shown in the examples of Section 4, for observed images, the higher the SNR the worse the image resolution. This may be contrary to our intuition, but the reason is simple. For bright sources, their influence on nearby object is strong, through convolution with a PSF, and the additive noise is weak. Therefore, the main beams of their CC curves will be broader. For high-quality observed images with high SNR, deconvolution can help improve the resolution, or even reach super-resolution results, as shown in Example II.

6 CONCLUSIONS

In this paper, a new definition of image resolution based on the correlation between pixels was introduced. For a series of observed images, the correlation is mainly due to the point spread functions of the imaging system, but is also influenced by the structures of the object and by any additive noise.

The resolution may vary across an image. The new definition is also suitable for the interpretation of

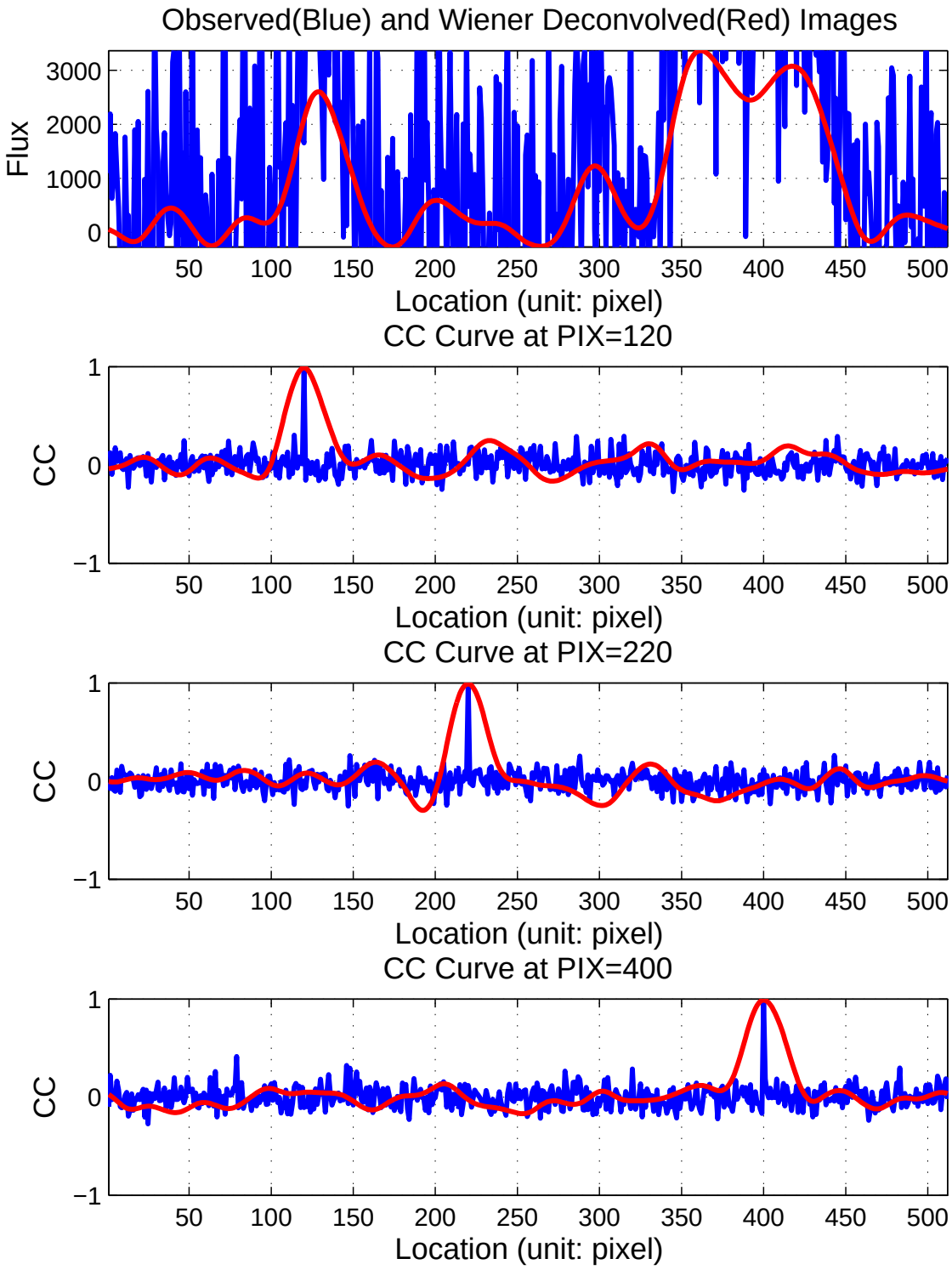

Fig. 10 Brightness distributions of an observed (blue) image and of its Wiener-deconvolved (red) image (top plot). The other plots show three pairs of CC curves , both for the observed (blue) and Wiener-deconvolved (red) image, for pixels 120 px, 220 px and 400 px respectively.

structures can be extracted from low signal-to-noise ratio data, but with low resolution; on the other hand

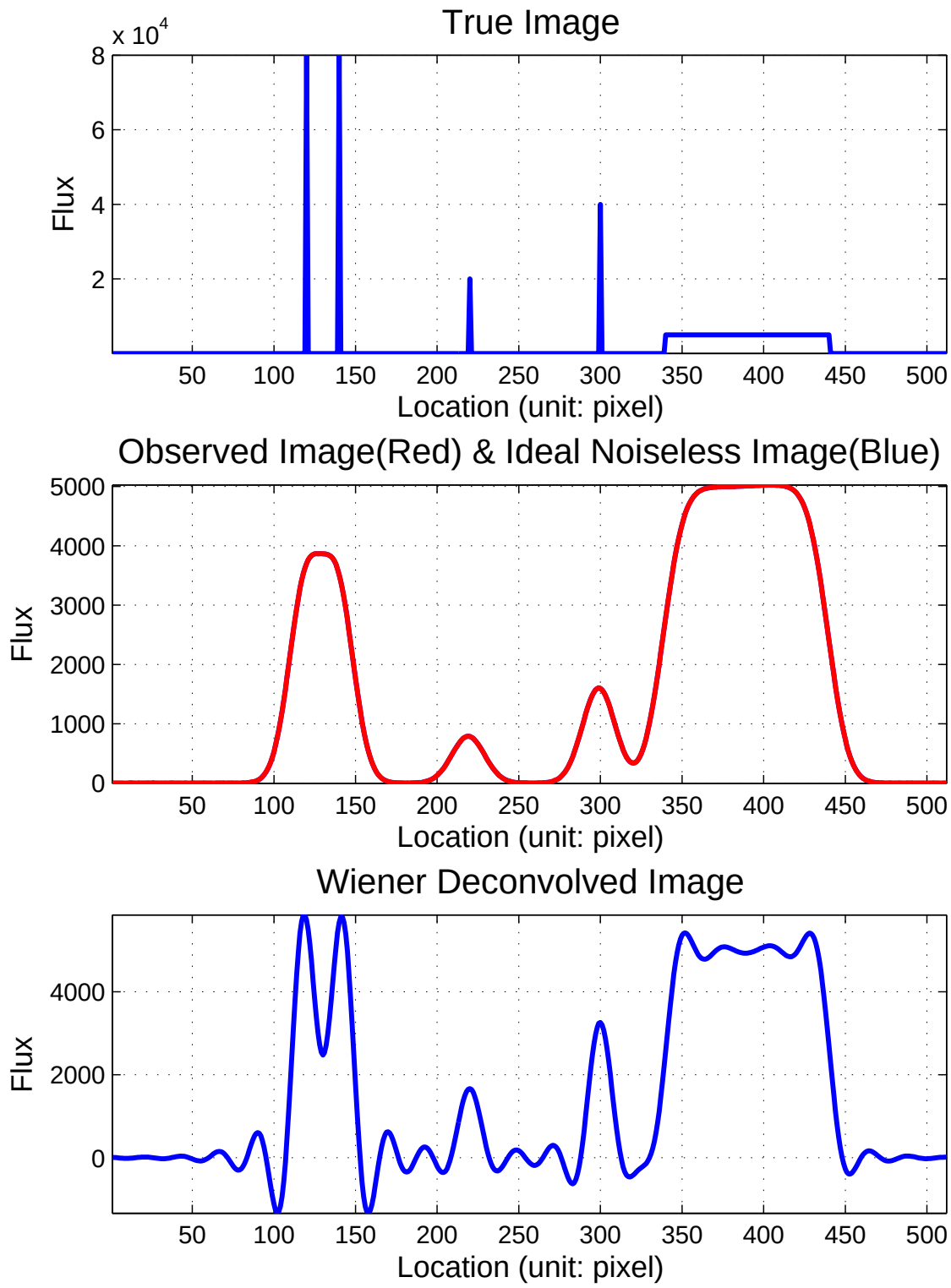

Fig. 11 The true image (top plot), the observed image as well as ideal noiseless image (middle plot) and Wiener deconvolved image (bottom plot) in Example II where the SNR of the observed image is about 930.

The new definition can also be used to compare various deconvolution algorithms on the effect of their

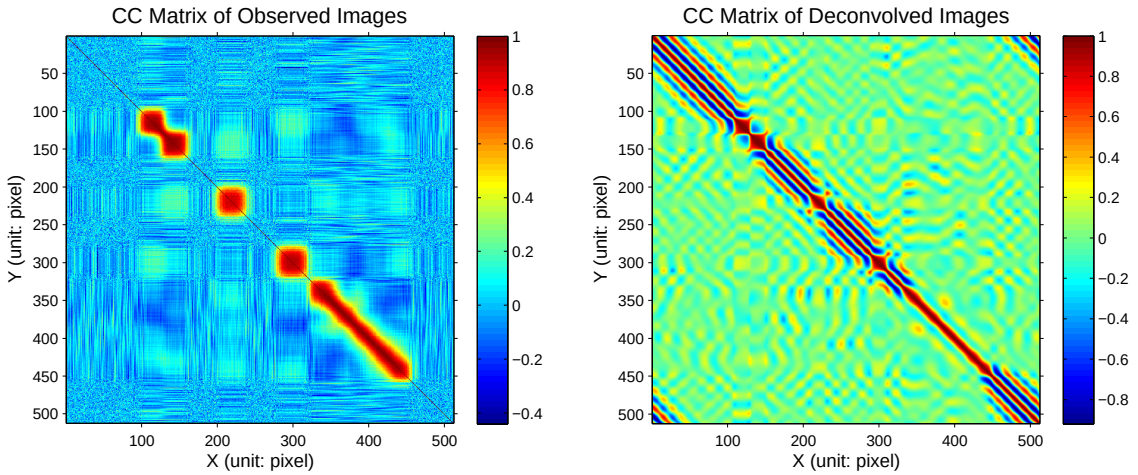

Fig. 12 The CC matrices of observed images (left plot) and deconvolved images (right plot). The SNRs of the observed images are about 930.

ACKNOWLEDGMENTS

This work was supported by the National Natural Science Foundation of China (NSFC) under Grant No. 11173038 and No. 11373025, and also by the Tsinghua University Initiative Scientific Research Program under Grant No. 20111081102. The author would like to thank Dr. Eric O. Lebigot for his kind help for the English improvement of this paper.

References

Akaike H., 1998, in Selected Papers of Hirotugu Akaike, Springer, p. 199
Banterle N., Bui K. H., Lemke E. A., and Beck M., 2013, Journal of structural biology, 183, 363
Blanter Y. M., Büttiker M., 2000, Physics reports, 336, 1
Born M., Wolf E., 1999, Principles of optics: electromagnetic theory of propagation, interference and diffraction of light, CUP Archive
Conchello J. A., JOSA A, 1998, 15, 2609
DeGroot M. H., 2005, Optimal statistical decisions, John Wiley & Sons, 82
Fried D. L., 1966, JOSA, 56, 1372
Högbom J., 1974, Astron. Astrophys. Suppl, 15, 417
Irani M., Peleg S., 1991, CVGIP: Graphical models and image processing, 53, 231
Jaynes E. T., 1957, Physical review, 106, 620
Janesick J. R., 2001, Scientific charge-coupled devices, SPIE press Bellingham, Washington, 117
Kalman R. E., 1960, Journal of Fluids Engineering, 82, 35
Labeyrie A., 1970, A & A, 6, 85
MacDonald L. W., 2006, Digital heritage: applying digital imaging to cultural heritage, Routledge
Nieuwenhuizen R. P., Lidke K. A., Bates M., Puig D. L., Grünwald D., Stallinga S., Rieger B., 2013, Nature methods, 10, 557
Pearson K., 1895, Proceedings of the Royal Society of London, 58, 240
Saxton W., Baumeister W., 1982, Journal of Microscopy, 127, 127
Tuzlukov V., 2010, Signal processing noise, CRC Press, 8
Ubertini P., Lebrun F. et al., 2003, A & A, 411, 131
Wiener N., 1949, Extrapolation, interpolation, and smoothing of stationary time series. MIT press Cambridge, MA, 2

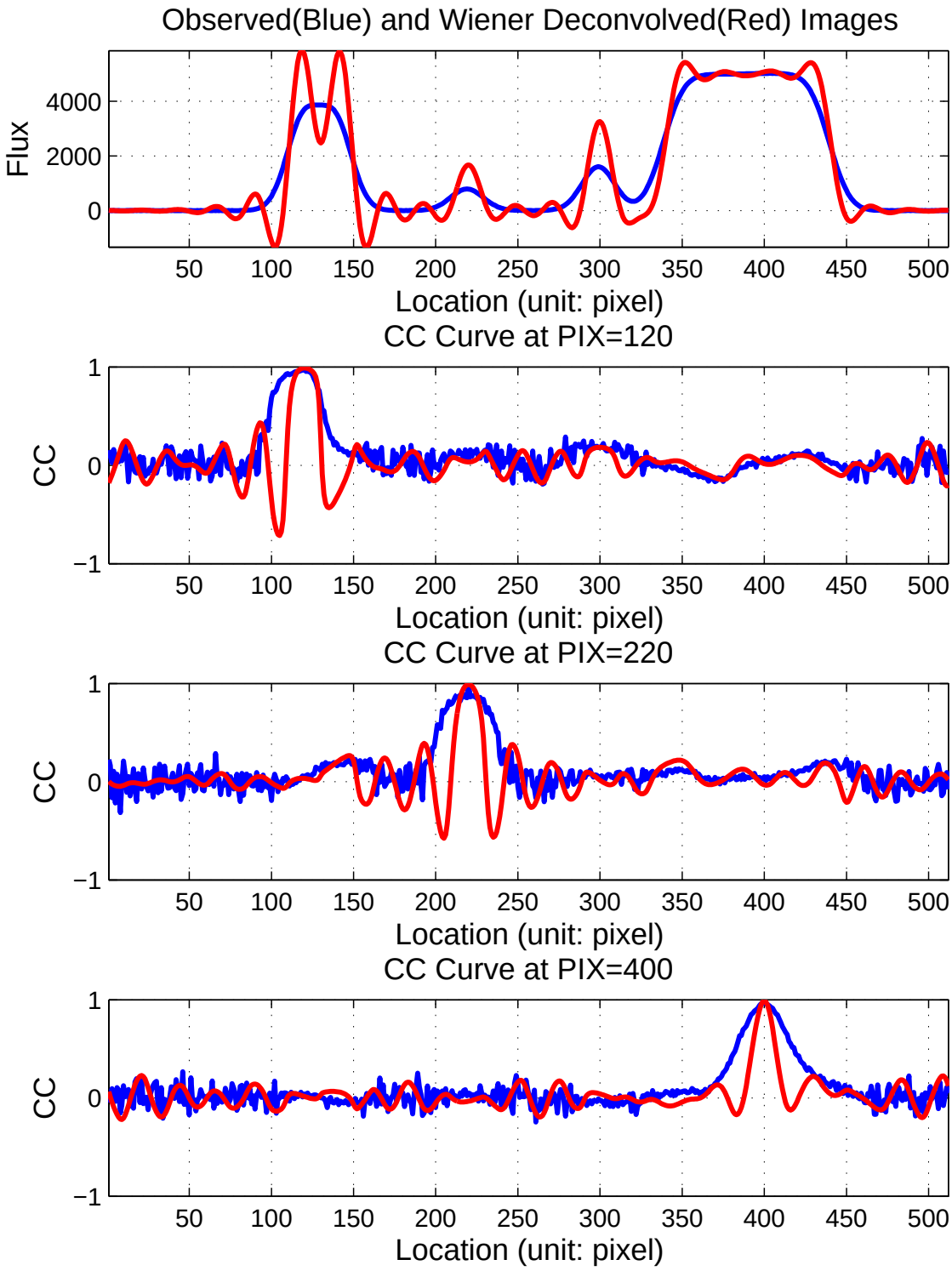

Fig. 13 The brightness distributions of an observed(blue) and a Wiener deconvolved(red) images (the 1st plot). Three pairs of CC curves (the 2nd, 3rd and 4th plots) related to observed (blue) and Wiener deconvolved (red) images at positions $120\,\mathrm{px}$, $220\,\mathrm{px}$ and $400\,\mathrm{px}$ respectively.